

Search for the Hawking radiation of primordial black holes: prospective sensitivity of LHAASO

Chen Yang,¹ Sai Wang,^{2,*} Meng-Lin Zhao,¹ and Xin Zhang^{1,3,4,†}

¹*Key Laboratory of Cosmology and Astrophysics (Liaoning Province) & Department of Physics,
College of Sciences, Northeastern University, Shenyang 110819, China*

²*Theoretical Physics Division, Institute of High Energy Physics,
Chinese Academy of Sciences, Beijing 100049, China*

³*National Frontiers Science Center for Industrial Intelligence and Systems Optimization,
Northeastern University, Shenyang 110819, China*

⁴*Key Laboratory of Data Analytics and Optimization
for Smart Industry (Northeastern University),
Ministry of Education, Shenyang 110819, China*

Primordial black holes (PBHs) with initial mass $\sim 5 \times 10^{14}$ g are evaporating due to Hawking radiation, leading to bursts of very-high-energy gamma rays. In this work, we investigate the prospective sensitivity of the Large High Altitude Air Shower Observatory (LHAASO) to measure the local burst rate density of PBHs. Our findings reveal that LHAASO is capable of searching for the PBH bursts within a distance ~ 0.1 pc from the sun and thereby measure the local burst rate density ~ 1164 (or 699) $\text{pc}^{-3} \text{yr}^{-1}$ at 99% confidence level during a 3 (or 5) year observing run. This stands for a sensitivity that is one order of magnitude stronger than the strongest observational constraint from the High Altitude Water Cherenkov Observatory (HAWC). In addition, we further suggest an observing strategy to search for the PBH bursts during upcoming observing runs of LHAASO.

I. INTRODUCTION

Being different from the astrophysical black holes as remnants of stellar evolution, the primordial black holes (PBHs) were produced in the early universe due to gravitational collapse of the enhanced cosmological curvature perturbations on small scales [1]. They have a wide mass range spanning from the Planck mass to several billions of solar mass, making them contribute to a variety of astrophysical phenomena. In particular, the PBH scenario was suggested to interpret the origin of stellar-mass binary black holes reported by the LIGO and Virgo Collaborations [2, 3]. Currently, the abundance of PBHs with respect to dark matter has been tightly constrained by a quantity of astronomical observations (for

* Corresponding author; wangsai@ihep.ac.cn

† Corresponding author; zhangxin@mail.neu.edu.cn

reviews see, e.g., Refs. [4, 5]). Further studies may hold the key to understanding both the origin of the early universe and the nature of dark matter.

As proposed by Steven Hawking in 1970s [6], a black hole can radiate in the blackbody spectrum with a thermal temperature inversely proportional to the black-hole mass. It would emit all species of fundamental particles that are approximately as massive as the thermal temperature [7, 8]. Based on theoretical estimate, Hawking radiation is nearly negligible for stellar-mass or more-massive black holes. In contrast, it would be essential for the evolution of less-massive black holes that are believed to be a smoking gun of PBHs, since the black holes in this mass range can be produced via the primordial process only, rather than the known astrophysical processes. In particular, at the present age of the universe, a short-duration burst would be involved for PBHs with initial mass $\sim 5 \times 10^{14}$ g [9]. Such a burst is expected to emit very-high-energy gamma rays in the GeV–TeV energy range, which may be detectable for the Large High Altitude Air Shower Observatory (LHAASO) [10].

It is important to search for the PBH bursts, no matter whether such bursts will be detected or not. Once these bursts are detected, we can not only prove the existence of PBHs and Hawking radiation, but also determine the local burst rate density of PBHs. If not, we will obtain stronger upper limits on the local burst rate density of PBHs. In whatever case, we could constrain the power spectrum of primordial density perturbations on much-smaller scales than those measured by the cosmic microwave background (CMB) [11], and then explore a variety of models of inflation. Besides these, a detection of PBH bursts can also inform quantum effects of gravity and particle physics beyond the energy scale achievable by the present-day Large Hadron Collider (LHC) [12], and the future Future Circular Collider (FCC) [13], Circular Electron Positron Collider (CEPC) [14], and International Linear Collider (ILC) [15].

In this work, we study the prospective sensitivity of LHAASO [10] in detection of the PBH bursts, which locate on parsec scales from the Earth. Several upper bounds have been placed on the local burst rate density of PBHs by the Whipple Atmospheric Cerenkov Telescopes (Whipple) [16], CYGNUS air-show arrays (CYGNUS) [17], High Energy Stereoscopic Systems (H.E.S.S.) [18], Tibet Air Shower Array [19], Milagro high energy observatorys (Milagro) [20], Very Energetic Radiation Imaging Telescope Array Systems (VERITAS) [21], Fermi Large Area Telescopes (Fermi LAT) [22], High Altitude Water Cherenkov Observatorys (HAWC) [23], and so on. Compared with these existing programs, LHAASO is sensitive to a wider energy range and has a higher sensitivity [10]. On the one hand, the detectable energy range of gamma rays is 30 GeV–100 PeV for LHAASO. The lower energy threshold allows for possible detection of PBH bursts at greater distances, and the higher energy bound opens up the field of very-high-energy gamma-ray astronomy beyond the currently observable bands. Furthermore, the sensitivity of LHAASO is significantly higher than the existing programs when the gamma-ray energy is greater than 10 TeV. Therefore, we expect this program to explore unknown territories via either placing the strongest upper limits on the local burst rate density of PBHs or getting the first detection of PBH bursts.

The remaining context of the paper is arranged as follows. In Section II, we show a brief summary of the theory of PBH bursts and the method of data analysis. In Section III, we obtain the prospective constraints from LHAASO on the local burst rate density of PBHs. In Section IV, the conclusions and discussion are presented.

II. PBH BURSTS: THEORY AND DATA ANALYSIS

In this section, we summarize the theory of PBH bursts and the method of data analysis.

A. Time-integrated number of photons per unit energy for an evaporating PBH

Throughout this work, we adopt the standard evaporation model, which indicates that the particles, emitted from PBHs due to Hawking radiation, exclusively consist of the particles in the Standard Model [7, 8]. The temperature T for a spinless PBH is inversely proportional to the mass M of this PBH, namely, $T = M_P^2/(8\pi M)$, where M_P denotes the Planck mass. As the PBH undergoes an evaporation process, its mass diminishes while its temperature escalates, leading to an increasing number of particle species and an increasing quantity of these particles. During the last stage of PBH evaporation, a notable outburst of particles is discharged, resulting in a burst event. The final particle products from such a burst include photons, electrons, protons, neutrinos, and their anti-particles. In this work, we focus on the very-high-energy gamma rays, which are potentially detectable for LHAASO.

In order to express the time-integrated number of photons per unit energy, it is convenient to represent the PBH temperature in terms of the PBH burst duration τ , corresponding to the PBH remaining lifetime, i.e., [24]

$$T \simeq 7.8 \times 10^3 \times \left(\frac{1 \text{ s}}{\tau}\right)^{\frac{1}{3}} \text{ GeV} . \quad (1)$$

Considering the observational energy range of LHAASO [10], we focus on an energy range $T > 10 \text{ GeV}$ in this work and take into account both of the primary and secondary particles. During the burst duration of a given PBH, the time-integrated number of photons per unit energy is approximated to be [25]

$$\frac{dN_\gamma}{dE}(E; \tau) \approx 9 \times 10^{35} \times \begin{cases} \left(\frac{1 \text{ GeV}}{T}\right)^{\frac{3}{2}} \left(\frac{1 \text{ GeV}}{E}\right)^{\frac{3}{2}} \text{ GeV}^{-1} & \text{for } E < T, \\ \left(\frac{1 \text{ GeV}}{E}\right)^3 \text{ GeV}^{-1} & \text{for } E \geq T, \end{cases} \quad (2)$$

where E is the energy of photons, T is related with τ via Eq. (1), and N_γ stands for the time-integrated number of photons.

B. Data analysis

Assuming that a PBH burst locates in the field of view of a given detector, we expect the total number of photons received by the detector to be

$$\mu(r, \theta_i, \tau) = \frac{(1-f)}{4\pi r^2} \int_{E_1}^{E_2} \frac{dN_\gamma}{dE}(E; \tau) A_\gamma(E, \theta_i) dE , \quad (3)$$

where r is the distance from the detector to the burst, θ_i is the zenith angle of band i , f is the dead-time fraction of the detector,¹ and A_γ is the effective area of photons. In addition, we assume that the duration of PBH burst is so short that all particles come from a zenith angle of the same band, without the necessity to consider the Earth's spin which should be considered when searching for a long-lasting burst.

To claim a detection of PBH bursts or otherwise place upper limits on the local burst rate density, we should find a minimum number of photons $\mu_{\min}(\theta_i, \tau)$, which is a threshold for claiming an excess over the background at 5σ confidence level. Firstly, we have N_t trials, i.e., [26]

$$N_t = \frac{S}{\tau} \left(\frac{\theta_{\text{fov}}}{\theta_{\text{res}}} \right)^2 , \quad (4)$$

where S is an observation duration, and θ_{fov} and θ_{res} denote the field-of-view and angular resolution, respectively, of the detector. Secondly, considering a correction for N_t trials, we define such a 5σ detection to be the number of counts n having a Poisson probability P that corresponds to a post-trial p-value

$$p_c = \frac{p_0}{N_t} = P(\geq n | n_{\text{bk}}) , \quad (5)$$

where $p_0 = 2.3 \times 10^{-7}$ is a pre-trial p-value that corresponds to 5σ . Here, $P(\geq k | m)$ is a Poisson probability of getting at least k counts when the Poisson mean is m . The number of background counts is n_{bk} , which is a product of the burst duration τ and the background rate $R_b(\theta_i)$, i.e.,

$$n_{\text{bk}} = \tau R_b(\theta_i) . \quad (6)$$

Here, the background rate is given by [20]

$$R_b(\theta_i) = \int_{E_1}^{E_2} \frac{dN_p}{dE}(E) A_p(E, \theta_i) dE \times [2\pi(1 - \cos \theta_{\text{res}})] \times 1.2 , \quad (7)$$

where A_p stands for the effective area of protons with E being the energy of protons, the cosmic ray (i.e., proton) spectrum is given by [27]

$$\frac{dN_p}{dE}(E) = 7900 \times \left(\frac{E}{1 \text{ GeV}} \right)^{-2.65} \text{ m}^{-2} \text{s}^{-1} \text{sr}^{-1} \text{GeV}^{-1} , \quad (8)$$

¹ Throughout this work, we disregard effects of the dead-time fraction via fixing $f = 0$.

and a correction factor of 1.2 accounts for the effect of other cosmic ray particles on the background. Finally, $\mu_{\min}(\theta_i, \tau)$ is related with a 50% Poisson probability of detecting a 5σ excess. This indicates that we can get $\mu_{\min}(\theta_i, \tau)$ by solving

$$P(\geq n | n_{\text{bk}} + \mu_{\min}(\theta_i, \tau)) = 0.5 , \quad (9)$$

which means that a Poisson probability P of getting at least n counts is 50%.

Letting the left hand side of Eq. (3) to equal $\mu_{\min}(\theta_i, \tau)$, we determine the maximum distance from which the PBH burst can be detected by the detector, i.e.,

$$r_{\max}(\theta_i, \tau) = \left[\frac{(1-f)}{4\pi\mu_{\min}(\theta_i, \tau)} \int_{E_1}^{E_2} \frac{dN_\gamma}{dE}(E; \tau) A_\gamma(E, \theta_i) dE \right]^{\frac{1}{2}} . \quad (10)$$

Therefore, an effective detectable volume for the detector is given by

$$V(\tau) = \sum_i V(\theta_i, \tau) = \frac{4}{3}\pi \sum_i r_{\max}^3(\theta_i, \tau) \frac{\text{FOV}(\theta_i)}{4\pi} , \quad (11)$$

where a solid angle corresponding to the field of view associated with the band i is

$$\text{FOV}(\theta_i) = 2\pi (\cos\theta_{i,\min} - \cos\theta_{i,\max}) . \quad (12)$$

Here, $\theta_{i,\min}$ and $\theta_{i,\max}$ stand for the minimum and maximum zenith angles of band i , respectively.

To find an upper limit on the local burst rate density, we assume that PBHs distribute uniformly in the neighborhood of our sun. The Poisson probability for a null detection is $P(0|m) = 1 - P(n \geq 1|m) = 1 - X = m^0 e^{-m} / 0!$, where m is the upper limit on the expected number of PBH bursts at X confidence level. When considering $X = 99\%$, we get $m = \ln 100 \approx 4.6$. This result leads to the 99% confidence level upper limit on the local burst rate density of PBHs, i.e., [20]

$$\text{UL}_{99} = \frac{4.6}{V \times S} , \quad (13)$$

which would be adopted to studies in the next section. As mentioned above, V and S stand for the effective detectable volume and the observation duration, respectively.

III. PROSPECTIVE SENSITIVITY OF LHAASO TO DETECT PBH BURSTS

In this section, we show the expected constraints from LHAASO on the burst rate density of PBHs in the neighborhood of our sun and further suggest an observing strategy to search for the PBH bursts in an upcoming observing run of LHAASO.

The LHAASO project is comprised of two detectors, i.e., the water cherenkov detector array (WCDA) and the square kilometer array (KM2A) [10]. The effective areas of photons

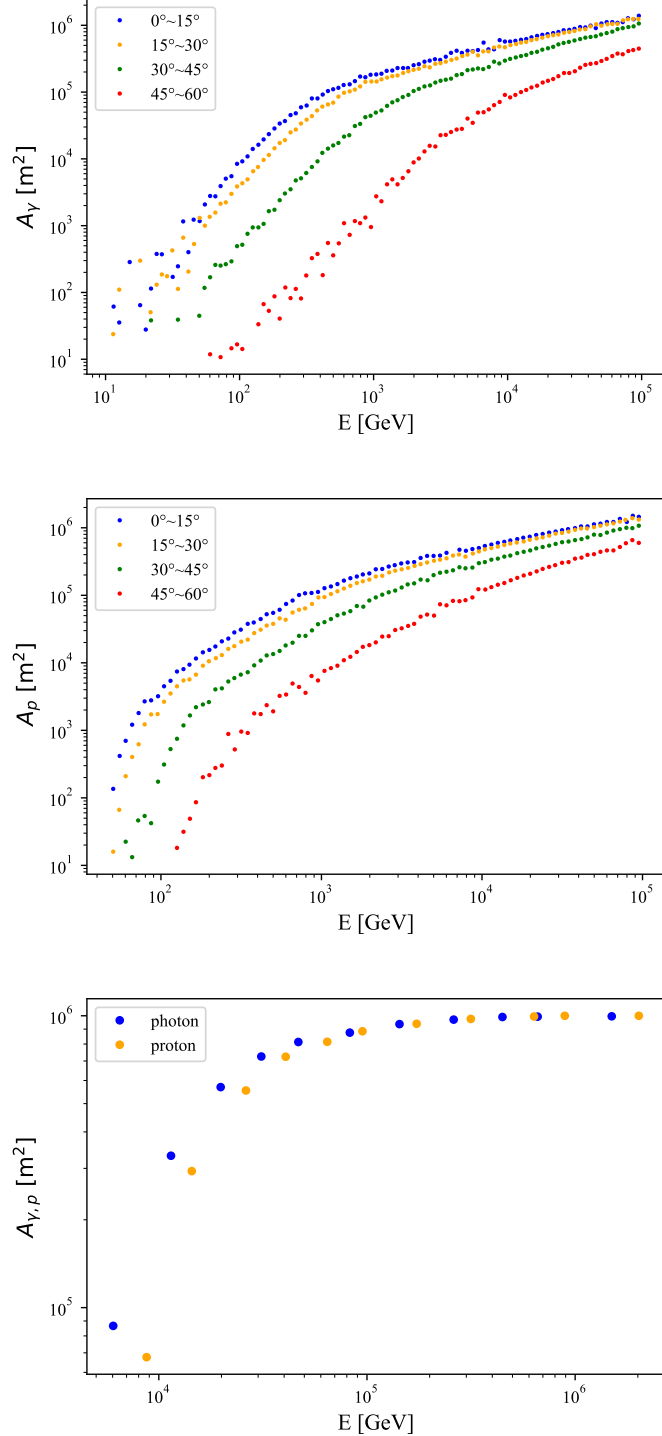


FIG. 1. Effective areas of photons and protons with respect to the energy bands and zenith angular bands. For WCDA (the zenith angle between 0° and 60° is equally divided into four bands), we show the upper panel for photons and the middle panel for protons. For KM2A (the zenith angle between 0° and 45° has only one band), we show the bottom panel for both photons and protons. These panels are reproduced from Refs. [28, 29].

Det.	τ [s]	θ_i	N_t	n_{bk}	μ_{min}
WCDA	10^{-3}	$0^\circ - 15^\circ (\theta_1)$	3.1×10^{14}	0.29	14.7
	10^{-3}	$15^\circ - 30^\circ (\theta_2)$	3.1×10^{14}	0.19	12.8
	10^{-3}	$30^\circ - 45^\circ (\theta_3)$	3.1×10^{14}	0.07	10.9
	10^{-3}	$45^\circ - 60^\circ (\theta_4)$	3.1×10^{14}	0.01	8.0
	10^{-2}	$0^\circ - 15^\circ (\theta_1)$	3.1×10^{13}	2.93	27.1
	10^{-2}	$15^\circ - 30^\circ (\theta_2)$	3.1×10^{13}	1.92	24.1
	10^{-2}	$30^\circ - 45^\circ (\theta_3)$	3.1×10^{13}	0.65	17.4
	10^{-2}	$45^\circ - 60^\circ (\theta_4)$	3.1×10^{13}	0.11	10.9
	10^{-1}	$0^\circ - 15^\circ (\theta_1)$	3.1×10^{12}	29.35	61.6
	10^{-1}	$15^\circ - 30^\circ (\theta_2)$	3.1×10^{12}	19.21	51.8
	10^{-1}	$30^\circ - 45^\circ (\theta_3)$	3.1×10^{12}	6.49	34.5
	10^{-1}	$45^\circ - 60^\circ (\theta_4)$	3.1×10^{12}	1.13	19.9
	1	$0^\circ - 15^\circ (\theta_1)$	3.1×10^{11}	293.51	164.5
	1	$15^\circ - 30^\circ (\theta_2)$	3.1×10^{11}	192.13	134.9
	1	$30^\circ - 45^\circ (\theta_3)$	3.1×10^{11}	64.92	83.1
	1	$45^\circ - 60^\circ (\theta_4)$	3.1×10^{11}	11.34	40.7
KM2A	10	$0^\circ - 15^\circ (\theta_1)$	3.1×10^{10}	2935.14	484.9
	10	$15^\circ - 30^\circ (\theta_2)$	3.1×10^{10}	1921.32	393.7
	10	$30^\circ - 45^\circ (\theta_3)$	3.1×10^{10}	694.92	232.1
	10	$45^\circ - 60^\circ (\theta_4)$	3.1×10^{10}	113.36	102.6
	10^2	$0^\circ - 15^\circ (\theta_1)$	3.1×10^9	29351.4	1482.6
	10^2	$15^\circ - 30^\circ (\theta_2)$	3.1×10^9	19213.2	1198.8
	10^2	$30^\circ - 45^\circ (\theta_3)$	3.1×10^9	6949.18	696.2
	10^2	$45^\circ - 60^\circ (\theta_4)$	3.1×10^9	1133.61	294.4
KM2A	10^{-3}	$0^\circ - 45^\circ (\theta_1)$	3.9×10^{14}	0.00	6.0
	10^{-2}	$0^\circ - 45^\circ (\theta_1)$	3.9×10^{13}	0.01	7.0
	10^{-1}	$0^\circ - 45^\circ (\theta_1)$	3.9×10^{12}	0.11	10.9
	1	$0^\circ - 45^\circ (\theta_1)$	3.9×10^{11}	1.09	18.9
	10	$0^\circ - 45^\circ (\theta_1)$	3.9×10^{10}	10.90	38.1
	10^2	$0^\circ - 45^\circ (\theta_1)$	3.9×10^9	109.04	98.0

TABLE I. The minimum number of counts $\mu_{\text{min}}(\theta_i, \tau)$ required for a 5σ detection with 50% probability for a series of burst durations τ and zenith angle bands θ_i for WCDA and KM2A during a 3 year observing run. Here, we also show the number of trials N_t and the number of background counts n_{bk} .

and protons with respect to the zenith angle bands for WCDA can be found in Ref. [28], while those for KM2A can be found in Ref. [29]. We reproduce them in Fig. 1. The field of view and the angular resolution of WCDA are given by $\theta_{\text{fov}} = 120^\circ$ and $\theta_{\text{res}} = 2.1^\circ$, respectively, while those of KM2A are given by $\theta_{\text{fov}} = 90^\circ$ and $\theta_{\text{res}} = 1.4^\circ$, respectively. Based on these setups and following the method in Section II, we get the explicit results of N_t , n_{bk} , and μ_{min} for each zenith angle band for several τ 's by assuming a 3 year observing run. They are listed in Tab. I.

Det.	τ [s]	r_{max} [pc]	V [pc ³]	UL ₉₉ [pc ⁻³ yr ⁻¹]
WCDA	10^{-3}	0.088	0.000303	5061
	10^{-2}	0.111	0.000657	2334
	10^{-1}	0.124	0.000954	1608
	1	0.126	0.000986	1555
	10	0.118	0.000754	2033
	10^2	0.106	0.000471	3255
KM2A	10^{-3}	0.077	0.000280	5475
	10^{-2}	0.105	0.000861	1779
	10^{-1}	0.129	0.001317	1164
	1	0.120	0.001060	1447
	10	0.085	0.000390	3930
	10^2	0.053	0.000097	15874

TABLE II. The 99% confidence level upper limits on the local burst rate density of PBHs, i.e., UL₉₉, for WCDA and KM2A for a 3 year observing run. For the burst durations in Tab. I, we also show the maximum detectable distance r_{max} , which corresponds to the zenith angle band θ_1 in Tab. I, and the effective detectable volume V .

Further following the method in Section II and still assuming the 3 year observing run, we also obtain the explicit results of r_{max} (for θ_1), V , and UL₉₉ for the burst durations coinciding with those in Tab. I. They are listed in Tab. II. On the other hand, for 3 and 5 year observing runs, the expected upper limits on the local burst rate density of PBHs, i.e., UL₉₉, are depicted in Fig. 2. For comparison, we also depict the observational constraints from Whipple [16], CYGNUS [17], H.E.S.S. [18], Tibet Air Shower Array [19], Milagro [20], VERITAS [21], Fermi LAT [22], and HAWC [23]. We find that compared with these programs, LHAASO gets a better sensitivity in searching for the PBH bursts. After the 5 year observing run, it would improve the upper limit reported by HAWC, i.e., the best one to our knowledge, by one order of magnitude.

As shown in Fig. 2, the observing duration S is an unnegligible factor that impacts our expected constraints on the local burst rate density of PBHs. Though we focus on the

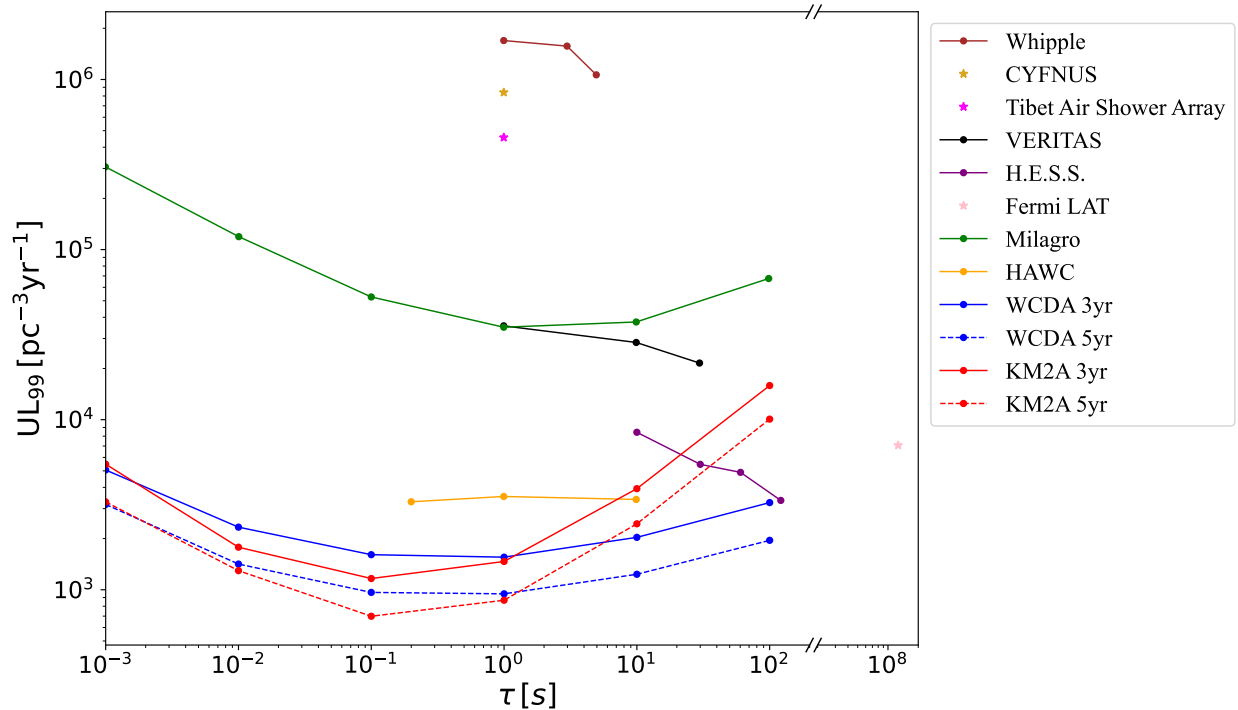


FIG. 2. The 99% confidence level upper limits on the local burst rate density of PBHs, i.e., UL_{99} , for WCDA and KM2A for 3 year and 5 year observing runs. Observational constraints at 99% confidence level from Whipple [16], CYGNUS [17], H.E.S.S. [18], Tibet Air Shower Array [19], Milagro [20], VERITAS [21], Fermi LAT [22], and HAWC [23] are shown for comparison.

observing duration of 3 years in Tab. I, μ_{\min} almost remains unchanged when considering other observing durations. In fact, it can be only modified by S in N_t . When considering other observing durations, e.g. 1 year or 10 years, we find that the post-trial probability in Eq. (5) changes only a few times. This would produce only a slight change to μ_{\min} [26]. Therefore, r_{\max} remains unchanged and thereby V also. Finally, though our results of UL_{99} , as shown in the last column of Tab. II, have been obtained by considering a 3 year observing run (i.e., blue solid curve for WCDA and red solid curve for KM2A), they can be adjusted to other observing durations by straightforwardly rescaling the value of S of Eq. (13). Correspondingly, we could also adjust the constraining curves in Fig. 2 for a quick estimate. To verify the above statement, we further show in Fig. 2 the exact results of UL_{99} for the 5 year observing run (i.e., blue dashed curve for WCDA and red dashed curve for KM2A), which coincide with the results from our quick estimate.

Finally, we emphasize that the search strategy of the PBH bursts is significantly impacted by the burst duration τ . It should be noted that compared with WCDA, KM2A is sensitive to a higher energy band [28, 29], which corresponds to a higher temperature of PBHs and thereby a shorter burst duration. This explains why WCDA is most sensitive to ~ 1 s bursts while KM2A is most sensitive to ~ 0.1 s bursts, as demonstrated in Fig. 2. In this sense, we

suggest that WCDA searches for the PBH bursts lasting for a burst duration $\sim 0.1 - 10$ s while KM2A searches for the PBH bursts lasting for a burst duration $\sim 0.01 - 1$ s. We leave a study of realistic data analysis to future works.

IV. CONCLUSIONS AND DISCUSSION

In this work, we have investigated the capability of LHAASO to search for the PBH bursts in the neighborhood of our sun. We obtained the expected sensitivities of two detectors, i.e., WCDA and KM2A, to measure the local burst rate density of PBHs. Our findings revealed that both detectors are capable of detecting the PBH bursts within a distance ~ 0.1 pc from the sun. Conversely, the null detection would lead to the upper limit on the local burst rate density of PBHs. For the 3 (or 5) year observing run of LHAASO, we could find the 99% confidence level upper limit to be ~ 1164 (or 699) $\text{pc}^{-3}\text{yr}^{-1}$, representing a sensitivity that is one order of magnitude stronger than the strongest observational constraint from HAWC. Considering the PBH burst duration, we proposed the observing strategies to search for the PBH bursts during the upcoming observing runs of LHAASO. To be specific, we suggested WCDA and KM2A, respectively, to search for the PBH bursts with remaining lifetimes $\sim 0.1 - 10$ s and $\sim 0.01 - 1$ s. Finally, we wish to further emphasize the importance to search for the PBH bursts. Actually, they are not only related with the quantum effects of gravity, but also related with the fundamental questions of cosmology, e.g., dark matter and origin of the cosmos.

As a concluding remark, we compare LHAASO with two future programs, namely, the Cherenkov Telescope Array (CTA) [30] and Southern Wide field of view Gamma-ray Observatory (SWGO) [31]. Though being limited by the size of the field of view, CTA can reach a larger r_{\max} due to its better sensitivity and thereby is expected to be still competitive with LHAASO. Due to having a wide field of view, SWGO was expected to measure the local burst rate density $\sim 50 \text{ pc}^{-3}\text{yr}^{-1}$ during a 10 year observing run [26]. This sensitivity is competitive with LHAASO. However, we emphasize that LHAASO monitors the northern hemisphere while SWGO monitors the southern hemisphere. They are complementary rather than competing.

ACKNOWLEDGMENTS

We thank Xiao-Jun Bi, Peng-Fei Yin, Shou-Shan Zhang, Xu-Kun Zhang, and Zhi-Chao Zhao for helpful discussions. This work is supported by the National SKA Program of China (Grant Nos. 2022SKA0110200 and 2022SKA0110203), the National Natural Science Foundation of China (Grant Nos. 12175243, 11975072 and 11835009), the National Key R&D Program of China (Grant No. 2023YFC2206403), the Science Research Grants from

the China Manned Space Project (Grant No. CMS-CSST-2021-B01), and the Key Research Program of the Chinese Academy of Sciences (Grant No. XDPB15).

[1] S. Hawking, *Mon. Not. Roy. Astron. Soc.* **152**, 75 (1971).

[2] M. Sasaki, T. Suyama, T. Tanaka, and S. Yokoyama, *Phys. Rev. Lett.* **117**, 061101 (2016), [Erratum: *Phys. Rev. Lett.* 121, 059901 (2018)], 1603.08338.

[3] Y. Ali-Haïmoud, E. D. Kovetz, and M. Kamionkowski, *Phys. Rev. D* **96**, 123523 (2017), 1709.06576.

[4] B. Carr, K. Kohri, Y. Sendouda, and J. Yokoyama, *Rept. Prog. Phys.* **84**, 116902 (2021), 2002.12778.

[5] B. Carr and F. Kuhnel, *SciPost Phys. Lect. Notes* **48**, 1 (2022), 2110.02821.

[6] S. W. Hawking, *Nature* **248**, 30 (1974).

[7] J. H. MacGibbon and B. R. Webber, *Phys. Rev. D* **41**, 3052 (1990).

[8] J. H. MacGibbon, *Phys. Rev. D* **44**, 376 (1991).

[9] T. N. Ukwatta, D. R. Stump, J. T. Linnemann, J. H. MacGibbon, S. S. Marinelli, T. Yapici, and K. Tollefson, *Astropart. Phys.* **80**, 90 (2016), 1510.04372.

[10] A. Addazi et al. (LHAASO), *Chin. Phys. C* **46**, 035001 (2022), 1905.02773.

[11] S. Wang, T. Terada, and K. Kohri, *Phys. Rev. D* **99**, 103531 (2019), [Erratum: *Phys. Rev. D* 101, 069901 (2020)], 1903.05924.

[12] *JINST* **3**, S08001 (2008).

[13] A. Abada et al. (FCC), *Eur. Phys. J. C* **79**, 474 (2019).

[14] M. Dong et al. (CEPC Study Group) (2018), 1811.10545.

[15] (2013), 1306.6352.

[16] E. T. Linton et al., *JCAP* **01**, 013 (2006).

[17] D. E. Andreas et al., *Phys. Rev. Lett.* **71**, 2524 (1993).

[18] F. Aharonian et al. (H.E.S.S.), *JCAP* **04**, 040 (2023), 2303.12855.

[19] Amenomori, M and Cao, Z and Dai, BZ and Ding, LK and Feng, YX and Feng, ZY and Hibino, K and Hotta, N and Huang, Q and Huo, AX and others, in *24th International Cosmic Ray Conference* (1995), vol. 2, p. 112.

[20] A. A. Abdo et al., *Astropart. Phys.* **64**, 4 (2015), 1407.1686.

[21] S. Archambault (VERITAS), *PoS ICRC2017*, 691 (2018), 1709.00307.

[22] M. Ackermann et al. (Fermi-LAT), *Astrophys. J.* **857**, 49 (2018), 1802.00100.

[23] A. Albert et al. (HAWC), *JCAP* **04**, 026 (2020), 1911.04356.

[24] F. Halzen, E. Zas, J. H. MacGibbon, and T. C. Weekes, *Nature* **353**, 807 (1991).

[25] V. B. Petkov et al., *Astron. Lett.* **34**, 509 (2008), 0808.3093.

[26] R. López-Coto, M. Doro, A. de Angelis, M. Mariotti, and J. P. Harding, *JCAP* **08**, 040 (2021), 2103.16895.

- [27] A. D. Panov et al., Bull. Russ. Acad. Sci. Phys. **71**, 494 (2007), astro-ph/0612377.
- [28] X.-Y. Wang, X.-J. Bi, Z. Cao, P. Vallania, H.-R. Wu, D.-H. Yan, and Q. Yuan, Chin. Phys. C **46**, 030003 (2022).
- [29] S. Cui, Y. Liu, Y. Liu, and X. Ma (LHAASO), Astropart. Phys. **54**, 86 (2014).
- [30] B. S. Acharya et al. (CTA Consortium), *Science with the Cherenkov Telescope Array* (WSP, 2018), ISBN 978-981-327-008-4, 1709.07997.
- [31] A. Albert et al. (2019), 1902.08429.